Published in the Proceedings of the 16th International Aluminum Alloys Conference (ICAA16) 2018
ISBN: 978-1-926872-41-4
by the Canadian Institute of Mining, Metallurgy & Petroleum

EXPERIENCE IN THE LOW PRESSURE CASTING IN PRINTED MOLDS OF A THIN BLADED ALUMINUM A356 IMPELLER

F. Chiesa[1,4], B. Duchesne[2], G. Morin, B. Tougas[1,4], N. Giguère[1,4], Jocelyn Baril[3]

[1]*Centre de Métallurgie du Québec (CMQ)*
Trois-Rivières, Québec, Canada
(Corresponding author: franco.chiesa@cegeptr.qc.ca)

[2]*Cegep de Trois-Rivières*
Trois-Rivières, Québec, Canada

[3]*Technologie du Magnésium et de l'Aluminium*
Trois-Rivières, Québec, Canada

[4]*REGAL Aluminium Research Centre*

ABSTRACT

An aluminum A356 compressor impeller was sand cast using the Low Pressure technique. The casting was limited in size (170 mm in diameter, 1.2 kg in weight) and very intricate in shape thus making 3D mold printing particularly favorable; indeed, producing this part by the traditional pattern-core box route would involve mounting 12 cores inside the mold while stringent dimensional tolerances are required as the impeller blades are only 2 mm thick. Consequently the molds were produce on the X-One MFlex printer of Quebec Metallurgy Center - CMQ. A dozen castings were produced with different casting temperatures and filling times so that it was possible to assess under which conditions complete filling of the mold cavity would be achieved. Filling and solidification modeling allowed predicting misruns and metallurgical properties inside the A356 (AlSi7Mg04) casting.

KEYWORDS

Aluminium, 3D mold printing, Additive manufacturing, Low pressure Sand casting, Modeling, Thin wall

INTRODUCTION

Recent advancements in additive manufacturing enable foundries to produce molds without the tooling (pattern and core boxes) necessary when conventional technology is used (Eyad, 2016). This is particularly advantageous when dealing with intricate shapes and/or when a limited number of parts must be produced within a few days rather than in 5 weeks. An additional advantage is gained when producing prototypes (Johnson, 2016) as changes are much less costly and time consuming when made on a numerical 3D drawing rather than on patterns and core boxes. 3D printing is normally economical for a small number of parts; however, if the part is not too big and very intricate in shape such as the part that will be studied in the present work, 3D printing can be economical even for an important number of castings to be produced.

On the other hand, low pressure casting is a high integrity casting process in which the mold cavity is filled from the bottom via a transfer tube in which the liquid aluminum rises under the pressure applied at the surface of the melt as illustrated in Figure 1. The filling can thus be precisely controlled, eliminating the turbulence created when the mold is filled from the top (gravity casting). Also, the pressure applied on the melt during solidification results in excellent feeding of the casting when conditions of directional solidification are met. In the present work, the compressor impeller shown in Figure 2 will be sand cast by low pressure.

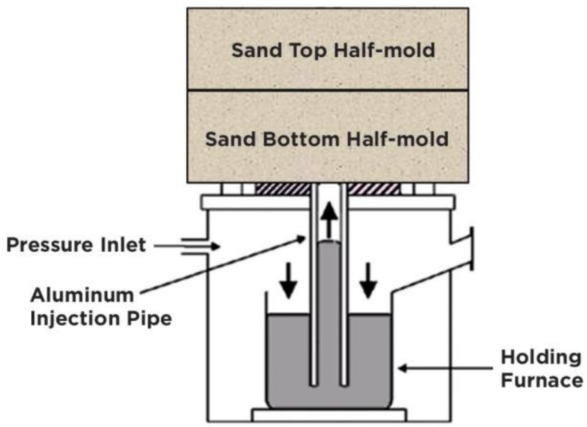

Figure 1. Principle of the low pressure casting

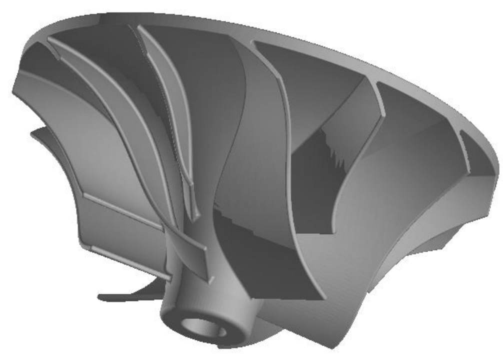

Figure 2. Impeller 170 mm in diameter, 80mm high

The low pressure casting process is also known for its ability to fill thin walls both in its permanent and sand mold versions. Figure 3 shows a 400 mm long grid originally machined, substituted by a LPPM cast part at a 75% cost saving (Chiesa, 2009); filling the 6 mm branches could not have been achieved by gravity casting. Figure 4 shows an exceptionally thin walled 5 kg, 550 mm high aeronautical air intake, 1.7 mm in wall thickness obtained by the low pressure sand casting process.

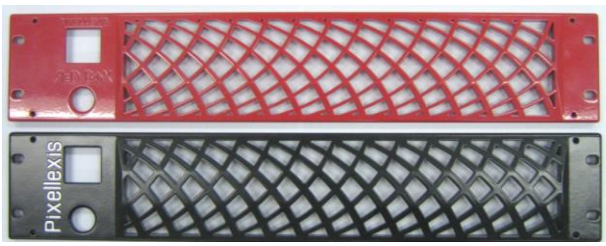

Figure 3. Housing grid cast (top) vs machined (bottom)

Figure 4. Air intake, 1.7 mm in wall thickness

SCOPE OF THE PRESENT WORK

The objective of this study is to test the thin wall capability of the low-pressure process by casting the aluminium A356 impeller shown in Figure 2, with 2 mm thick blades. The bulk of the work will be experimental. However, filling and solidification modeling will be used to compare the actual occurrence of misruns with the prediction. Solidification modeling will also be used to predict the metallurgical quality (dendrite fineness, DAS and porosity level) and the tensile properties of the casting in the T6 condition. The techno-economical advantages of mold printing for casting the A356 impeller shown in Figure 2 will be assessed. The casting under consideration lends itself particularly well to the use of 3D printing, because of its relatively small size, along with the complexity associated with assembling 12 cores to be accurately located in the mold when choosing the traditional pattern/core box route.

PRODUCING THE LOW PRESSURE MOLDS ON THE X-ONE MFLEX PRINTER

The 12 molds were produced on the binder jetting printer shown in Figure 5.

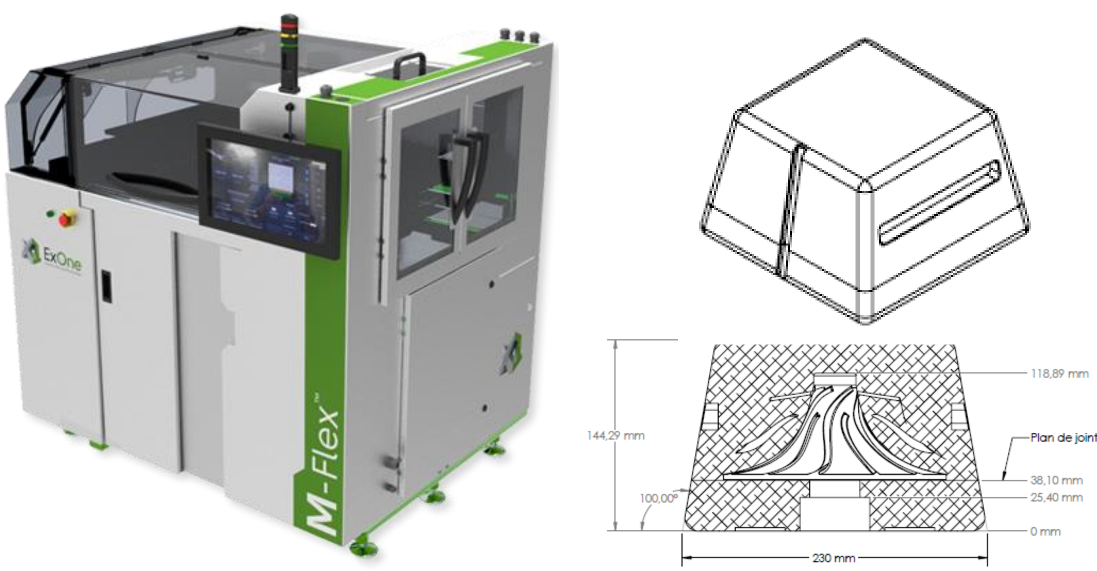

Figure 5. The EX ONE printer and mold to be produced

The silica sand, deposited in 250 µm thick layers, had the size distribution shown in Figure 6. In spite of fineness of the sand (82.2 AFS), the permeability of the mold was very high (180 to 220 AFS) due to the narrow distribution. Tensile strength was measured to be 182 psi in 1” × 1” dogbone samples with a standard deviation of 32 psi. The binder content, measured by the loss on ignition, was on the high side in the range of 2.3–2.5%.

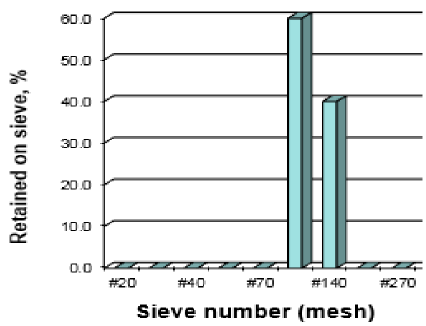

Figure 6. Mold silica sand narrow distribution

Casting by Low Pressure

The 11 molds shown in Figure 7 were cast by low pressure. The molds were accurately positioned and secured on the low pressure casting machine platen as shown in Figure 8. Out of curiosity, Mold # 12 was poured by gravity, directly into the mold cavity (i.e. without gating), an unorthodox technique bound to produce a poor metallurgical quality (high turbulence leading to extensive oxidation).

Figure 7. Molds with inserted thermocouples

Figure 8. Mold ready to be cast on LP machine

Two thermocouples were inserted at the bottom and top of the molds (Figure 9) in order to measure the casting temperature and to check that the filling time did correspond to the slope of the pressure curve. A typical pressure curve is shown in Figure 10, where the first ramp (0 to 10 s) brings the metal up the transfer tube; a 5 s pause is then observed, followed by a 10 mB/s ramp, which corresponds to a liquid aluminum rise of 40 mm/s, and a filling time of 2 seconds given the casting height of 80 mm. The response of the thermocouple confirmed that the measured filling time did match the calculated one even for very fast filling. This means than no pressure builds up in the mold thanks to the high permeability of the sand.

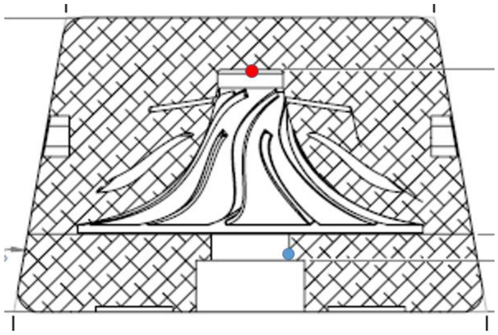

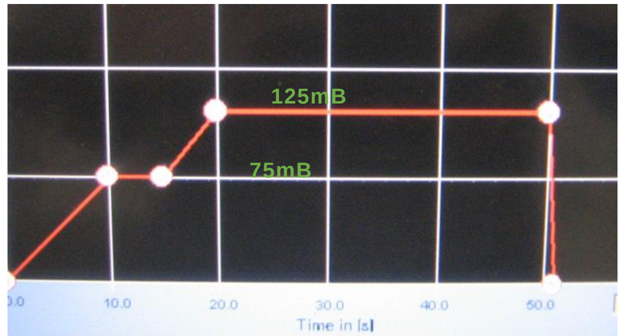

Figure 9. Location of the 2 thermocouples (dots) Figure 10. Rise in pressure for a filling time of 2 seconds

The A356.2 alloy obtained from primary aluminum ingots was grain refined by adding 20 ppm of boron via an Al 5Ti 1B master alloy; it was not modified. Its composition is given in Table 1.

Table 1. Composition of the alloy obtained from clean primary ingots (beginning of run)

Mass %	Si	Fe	Cu	Mn	Mg	Zn	Cr	Ti	Sr
Alloy A356	7.14	0.12	0.03	0.02	0.34	0.04	0.01	0.10	< 0.01

The melt was thoroughly degassed for 15 min with argon, down to a Reduced Pressure Test (RPT) sample density of 2.60 corresponding to a low hydrogen content of 0.1 ppm (Mulazimoglu, 1989). The 400 grit polished surfaces of the RPT samples at the beginning and at the end of the run are shown in Figure 11.

Figure 11. Reduced pressure test samples at the beginning (after degassing) and end of the casting trials

Observations About the Castings Produced

The castings at shake out are shown in Figure 12 and the casting conditions are listed in Table 2 where the status indicates whether the casting was complete; a clean sand blasted casting is also shown (Casting #10). These results confirm a well known fact: The casting process is not perfectly reproducible. For intance, in spite of the fact that the parts and the filling exhibit a perfect cylindrical symmetry, the misruns observed in the blades do not show this symmetry at all. Another discrepancy is seen when comparing casting #4 and casting #10, both cast in 4 seconds. Casting # 4, with a pouring temperature of 680°C is incomplete while casting #10 poured at 675°C is complete. We also note that penetration of the metal into the sand took place for castings #5 and #11 due to a combination of relatively high pouring temperature (680 and 675°C) and a very fast filling in 2 seconds. Casting #12 was directly poured by gravity in an estimated 2 seconds, without the proper gating that would have been necessary to obtain good properties.

Mold printing results in a rather rough surface finish (300 rms) which could be improved by spraying a mold coating, a well-known practice in sand foundries.

Table 2. Casting conditions of castings #1 to #11 (low pressure) and casting #12 (gravity poured)

Mold number	Filling time	Pouring temp.	Status
	seconds	±2°C	
1	8	700	incomplete
2	8	700	incomplete
3	8	700	incomplete
4	4	680	almost compl.
5	2	680	complete
6	2	640	incomplete
7	4	670	almost compl.
8	2	655	less than 7
9	8	675	similar to 8
10	4	675	complete
11	2	675	complete
12 gravity	2	660	complete

Casting #10 (300 rms roughness)

From these experiments, it can be concluded that optimal conditions are obtained when filling the mold in 4 seconds with a pouring temperature of 700°C.

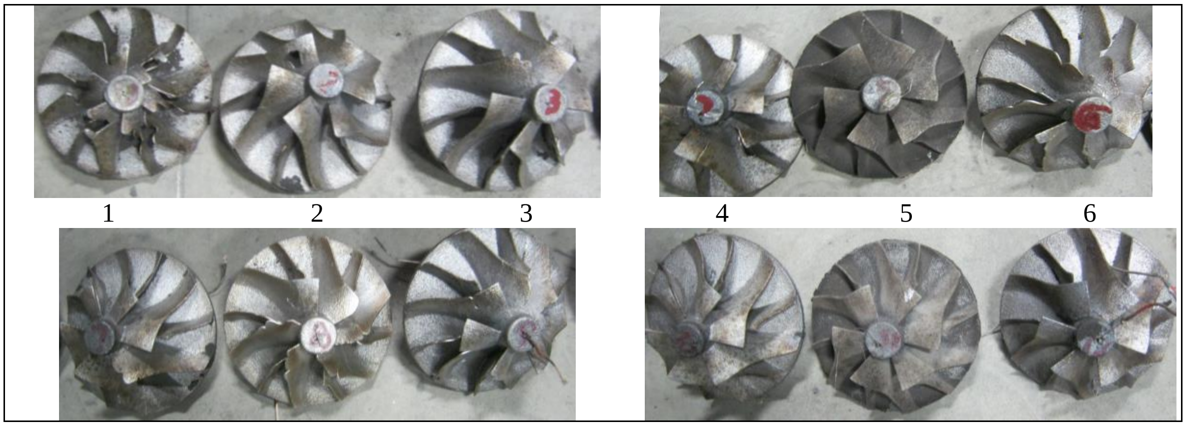

1 2 3 4 5 6

7 8 9 10 11 12

Figure 12. Castings #1 to #12 as obtained at shakeout for conditions of Table 2

MODELING FILLING

When modeling filling for the conditions of casting # 4 (680°C, filling in 4 s), the misruns predicted are shown in Figure 13, while the actual misruns are shown in Figure 14. The software predicts a misrun when the temperature of the liquid metal front reaches 607°C (i.e. 6°C below the liquidus temperature); this occurs on the side of the larger blades, while the observed misruns occur at the top of these larger blades. This discrepancy may be attributed to the fact that the software assumes a constant filling rate; in low pressure, it is the rise of the metal surface which is constant (4 mm/mB) rather than the flow rate. It makes that for the present part geometry, the flow rate is very high at the beginning of the fill (due to the large horizontal cross section of the part) and is reduced by a factor of 6 at the end of filling as shown on the graph of Figure 15. For an accurate result, the software should be modified so that the actual flow rate should be input according to the data in Figure 15.

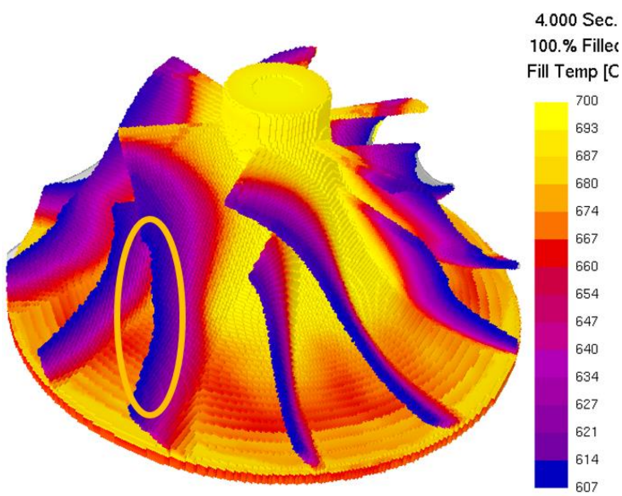

Figure 13. Location of the predicted misrun

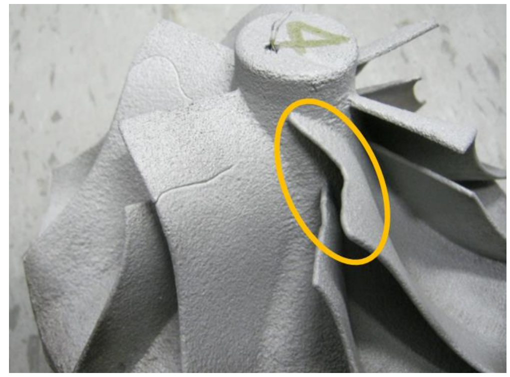

Figure 14. Photo of part showing actual misrun

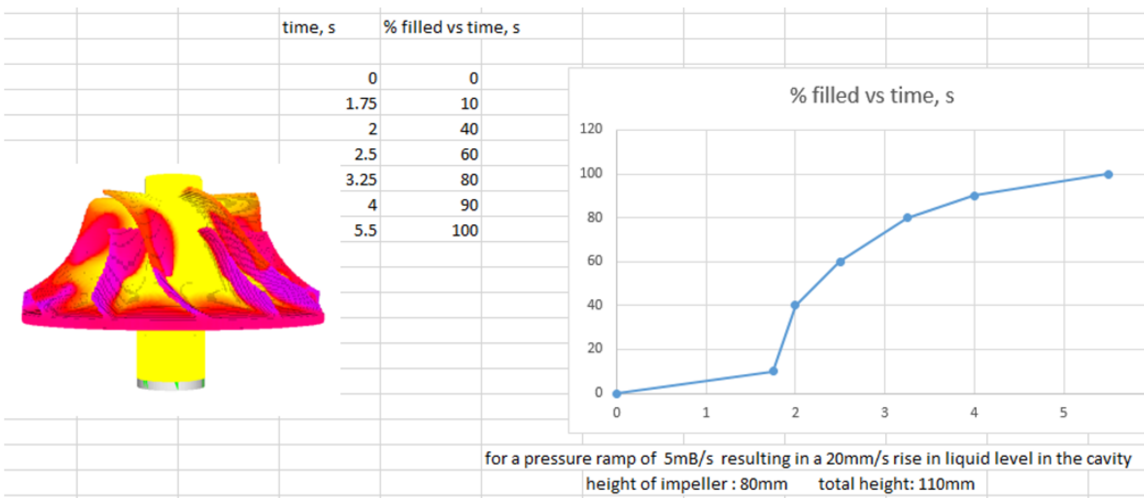

Figure 15. Rate of filling of the impeller for the geometry at hand. The flow rate is the slope of the curve

MODELING SOLIDIFICATION

When filling and solidification is modeled for a pouring temperature of 680°C and a filling time of 4 s, the solidification sequence in Figure 16 is obtained. It shows a clear directional solidification towards the bottom feeding tube, which should result in a basically shrink free casting.

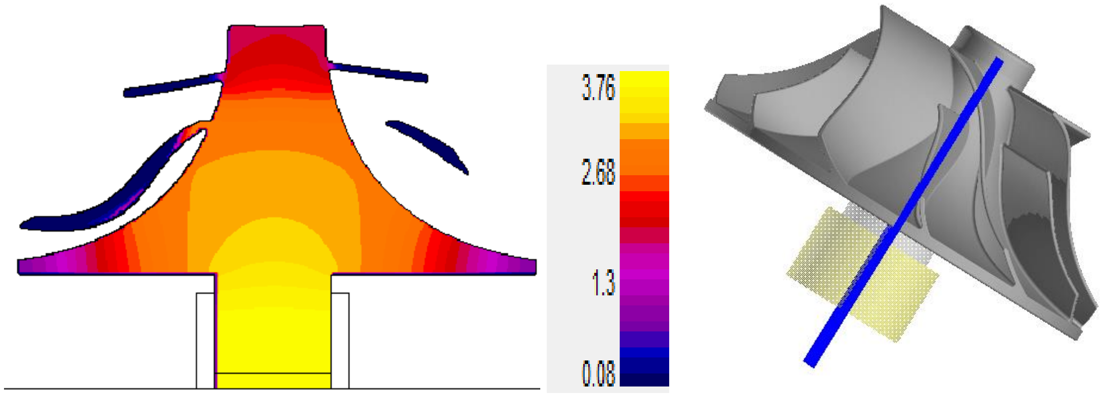

Figure 16. Progression of the solid metal front (in min) in a cross section of the impeller (blue line)

Prediction of Dendrite Fineness (DAS) and Microporosity Level

Earlier works have determined the relationships between DAS (µm) and solidification time (min) (Lee, 1990) and between porosity (vol %) and solidification time (min) and solidus velocity (cm/min) (Chiesa, 1999) for a melt degassed to 0.1 ppm. These thermal parameters are readily available everywhere in the casting via the simulation, so that the maps of Figure 17 can be obtained.

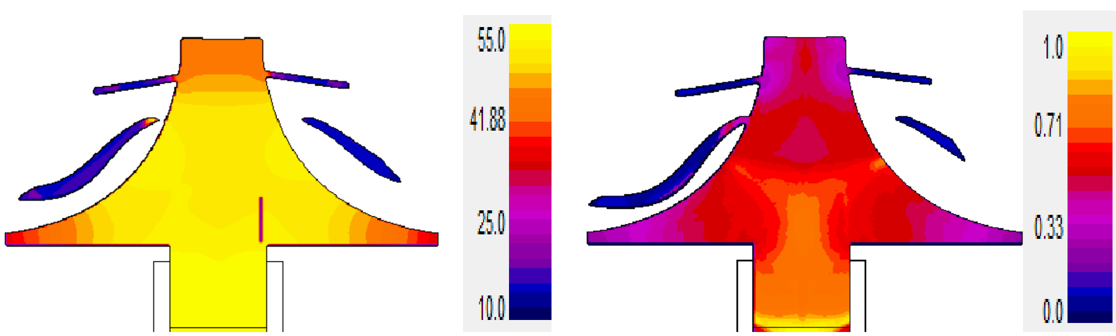

Figure 17. Distribution of DAS (µm) and microporosity (%) in a section of the impeller

The DAS vary considerably within the impeller, from less than 20 µm in the blades, to above 50 µm in the core of the casting. The microporosity level is everywhere less than 0.8%, insuring a radiographic level of quality corresponding to a Grade B level per ASTM B686.

Prediction of the Tensile Properties

The Centre Technique des Industries de la Fonderie (CTIF) has developed the concept of Quality index Q in AlSiMg alloys (Drouzy, 1980). When UTS is the ultimate tensile strength and El the elongation at break, Q (MPa) = UTS+150 Log El; Q only depends on the metallurgical quality and not on the temper applied to the heat treated AlSiMg alloy. On the other hand, the yield strength YS depends only on the magnesium content and the temper conditions (aging temperature and time following solutionizing) and not on the metallurgival quality (DAS, porosity). Combined with solidification modeling, their work lead to the possibility to predict the quality index Q in a casting (Chiesa, 2006), and YS, UTS and El if the magnesium content and temper conditions are known. When this is done for the impeller at hand, the quality index distribution of Figure 18 is obtained.

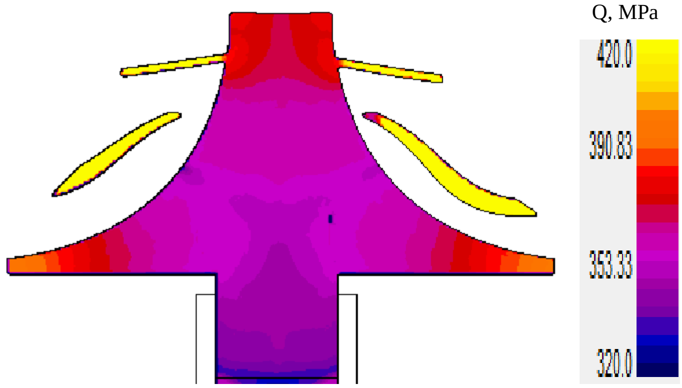

Predicted UTS and Elongation vs Q		
Mg=0.34%,	T6, aged for 6h at 160°C	
	YS=211 MPa	
Q, MPa	**UTS, MPa**	**El, %**
320	251	2.9
340	257	3.6
360	263	4.4
380	269	5.5
400	274	6.9
420	280	8.6

Figure 18. Map of the distribution of the Quality index (MPa) and related tensile properties (Table)

Since the magnesium content of the alloy and the aging conditons are known (indicated on top of the Table in Figure 18), the yield strength of the alloy may be obtained (Drouzy, 1980): 221 MPa. Since YS, UTS and El are correlated, the table on the right of Figure 18 can be obtained and a predicted value of UTS and El may be determined. Thus one can expect a minimum elongation of 4% in the core of the casting, and a maximum elongation of 7% in the blades.

Technical and Economic Considerations

The cost of a 3D printed mold is substantially higher than that of a mold produced via the traditional pattern/corebox route; however there is no pattern and core boxes to amortize. One may evaluate today's cost of the present impeller printed mold at 150$, while the cost of a traditional mold, including the production and mounting of 12 cores from 2 core boxes would only cost 35$. If the cost of the pattern and the 2 core boxes is 3000$, mold printing will still be more economical than the traditional process if less than 26 castings are to be produced. So, it is clearly the most economical and most suitable process for prototype production when modifications of the part can be expected which will require new patterns. From a technical point of view, mold printing provides a better dimensional accuracy but a poorer surface finish, which could be improved by spraying a coating on the surface of the mold cavity; however, it would still do not match the finish obtained by the traditional method.

CONCLUSIONS

3D printing of sand molds is becoming more and more popular; it is technically and economically viable. This is especially true for prototyping and small volume productions. The molds can be produced in only a few days instead of several weeks with conventional technologies. It is also possible to obtain very intricate parts which would be very difficult to produce with conventional technologies and would require a very large number of core packages. The combination of 3D printed sand molds together with the low pressure casting process allows the casting of very thin walled intricate components with excellent mechanical properties. Simulation techniques allow precise modeling of the casting process, prediction of possible errors and design optimization. The mechanical properties can also be predicted with fair accuracy. These technologies which are now available to foundries have a high potential to help the most innovative foundries to expand their business and enter new markets with new applications.

ACKNOWLEDGMENTS

The authors wish to acknowledge the financial support of Quebec Ministry of Education Technological research program (PART). They also recognize the valuable contribution of Justin Plante, intern student from the metallurgy department from Laval University, for carrying out the 3D printing and the sand tests.

REFERENCES

Chiesa, F., Duchesne, B., & Morin, G. (2006). Comparing prediction and measurement of the quality index in sand, permanent mould and investment castings poured in AlSi7Mg04 (A356). *Proceedings of the International Symposium on Aluminium: From Raw Materials to Applications*, CIMM Publications, 115–130.

Chiesa, F. & Mammen, J. (1999). Correlating microporosity to local solidification conditions and RPT in Aluminum A356 castings. *Transactions of the AFS*, *107*, 103–111.

Chiesa, F., Baril, J., & Dubé, P. (2009). Lights, camera, castings! *Engineered Casting Solutions, March–April*, 24–26

Drouzy, M., Jacob, S., & Richard, M (1980). Interpretation of tensile results by means of the Quality Index. *AFS International Cast Metal Journal, June*, 43–50.

Eyad, S. et al. (2016). Quantifying the role of part design complexity in using 3D sand printing for molds and cores. *International Journal of Metalcasting, 10*(3), 240–252.

Johnson O., Mueller, T., & Lindberg, M. (2016). Economic and timing benefits of 3D printed molds for prototype production castings. *Proceedings of the American Foundry Society*, paper 16-151, 6 p.

Lee, Y.W., Chang, E., & Chieu, C.F. (1990). Modeling of feeding behavior of solidifying Al-7Si-0.3Mg alloy plate castings. *Metallurgical Transactions, 21B*, 715–722.

Mulazimoglu, H.M., Handiak, N., & Gruzleski, J.E. (1989). Some observations on the reduced pressure test and hydrogen concentration of modified A356 alloy. *Transactions of the AFS, 97*, 225–232.